University of Baghdad
College of Engineering
JOURNAL OF ENGINEERING

Journal of Engineering

journal homepage: www.jcoeng.edu.iq
Number 3 Volume 24 March 2018

Civil and Architectural Engineering

Analysis of Double Skin Composite Slabs

Husain M. Husain
Professor

Mohannad H. Al-Sherrawi
Instructor

Asmaa Taha Ibrahim
Engineer

College of Eng. - University of Baghdad
mhnd7@yahoo.com

ABSTRACT

This paper deals with finite element modeling of the ultimate load behavior of double skin composite (DSC) slabs. In a DSC slab, shear connectors in the form of nut bolt technique studs are used to transfer shear between the outer skin made of steel plates and the concrete core. The current study is based on finite element analysis using ANSYS Version 11 APDL release computer program. Experimental programmes were carried out by the others, two simply supported DSC beams were tested until failure under a concentrated load applied at the center. These test specimens were analyzed by the finite element method and the analyses have shown that these slabs displayed a high degree of flexural characteristics, ultimate strength, and ductility. The close agreement has been observed between the finite element and experimental results for ultimate loads and load–deflection responses. The finite element model was thus found to be capable of predicting the behavior of DSC slabs accurately.

Keywords: DSC slabs; Shear studs; Ultimate load behavior; Finite element method; Steel-concrete-steel sandwich construction.

تحليل البلاطات المركبة ذات غطائين

أسماء طه إبراهيم
مهندس

مهند حسين الشراوي
مدرس

حسين محمد حسين
أستاذ

كلية الهندسة – جامعة بغداد

الخلاصة

يتناول هذا البحث التمثيل باستخدام العناصر المحددة لسلوك البلاطات الخرسانية المركبة ذات غطائين حديد عند الحمل الأقصى. في هكذا بلاطات ، تستخدم البراغي كروابط القص لنقل قوى القص بين غطائي الحديد واللب الخرساني. تستند الدراسة الحالية على تحليل العناصر المحددة باستخدام برنامج الحاسوب ANSYS إصدار APDL 11. باستعمال طريقة العناصر المحددة ، تم تحليل عتبين مسندين إسناد بسيط ، فحصا مختبريا من قبل آخرين تحت تأثير حمل مركز وإلى حد الفشل. وقد بينت نتائج التحليل أن هذه نماذج أظهرت درجة عالية من خصائص الانثناء والقوة القصوى واللدونة. وقد لوحظ وجود تقارب بين نتائج العناصر المحددة والنتائج التجريبية للأحمال النهائية وإستجابات الانحراف. وبهذا فقد وجد بأن طريقة العناصر المحددة قادرة على التنبؤ بسلوك البلاطات الخرسانية المركبة ذات غطائين حديد بدقة.

1. INTRODUCTION

Steel-concrete-steel sandwich (SCSS) construction or double skin composite (DSC) construction is a relatively new and innovative form of construction consisting of a layer of plain concrete, sandwiched between two layers of relatively thin steel plate, connected to the concrete by stud connectors as shown in Fig. (1). SCSS construction was originally conceived as an alternative form of construction for immersed tube tunnels 1-3 but has since been considered for a variety of, offshore and onshore applications including oil production and storage vessels, caissons, core shear walls in tall buildings and impact and blast resistant structures.

The perceived advantages of the system are that the external steel plates act as both primary reinforcement and permanent formwork, and as impermeable, impact and blast resistant membranes. The full depth stud connectors transfer normal and shearing forces between the concrete and steel plates and act as transverse shear reinforcement.

In this study, the comparison is made between the results obtained from the finite element analysis and the available experimental results in order to check the validity and accuracy of the finite element model. Thus, two specimens with available experimental results have been analyzed here and the finite element results are compared.

After that, a nonlinear three-dimensional finite element analysis has been used to predict the load-deflection behavior of a double skin composite slab consisting of a concrete slab sandwiched between two plates with shear connectors under uniformly distributed load using ANSYS computer program (Version 11, copyright 2007).

2. MATERIAL MODELING

2.1 Steel Plate

Steel plate material is assumed to behave as a bilinear uniaxial stress-strain relationship. The stress-strain diagram consists of two branches: A first branch starts from the origin with a slope equal to E_s, up to f_y. A second branch is horizontal or, for practical use of computers, is assumed to have a very small slope ($E_w \approx 0.02E_s$) as shown in Fig. (2).

The material coefficients to be adopted in calculations for the steels covered by this study have been taken, as follows, according to **EC4 1994**:

- Modulus of elasticity $E_s = 210000\ \text{N/mm}^2$
- Shear modulus $G_s = E_s /2\ (1+\upsilon_s)$
- Poisson's ratio $\upsilon_s = 0.3$

2.2 Concrete

The ANSYS computer program requires the uniaxial stress-strain relationship for concrete in compression. Numerical expressions, **Desayi** and **Krishnan**, **1964**, the following Eq. (1) and (2), were used along with Eq. (3), **Gere** and **Timoshenko**, **1997**, and Eq. (4), **ACI 318-14** to construct the uniaxial compressive stress-strain curve for concrete in this study.

$$f = \frac{E_c \varepsilon}{1+\left(\frac{\varepsilon}{\varepsilon_o}\right)^2} \quad (1)$$

$$\varepsilon_o = \frac{2f'_c}{E_c} \quad (2)$$

$$E_c = \frac{\sigma}{\varepsilon} \quad (3)$$

$$E_c = 4700\sqrt{f_c'} \quad (4)$$

where:
σ = stress at any strain ε, N/mm^2.
ε = strain at stress f .
ε_o = strain at the ultimate compressive strength f_c'.

It is important to mention that the stress-strain curves end at ultimate strain (ε_u) equal to 0.003 mm/mm. Fig. (3) shows the simplified compressive uniaxial stress-strain relationship that has been used in this study.

For concrete, ANSYS computer program requires following input data for material properties, **Kachlakev**, **et al.**, **2001**:

- Elastic modulus (E_c).
- Ultimate uniaxial compressive strength (f_c').
- Ultimate uniaxial tensile strength (modulus of rupture, f_r).
- Poisson's ratio (υ).
- Shear transfer coefficient for opened and closed cracks (β_o and β_c respectively).
- Compressive uniaxial stress-strain relationship for concrete.

From the ultimate uniaxial compressive strength (f_c'), obtained from appropriate standard tests, the elastic modulus of concrete (E_c) for each model was calculated according to ACI 318-14 by using Eq. (4). Poisson's ratio for concrete was assumed to be 0.2, **Bangash**, **1989**, for all sandwich slabs.

The shear transfer coefficient, β, represents conditions of the crack face. The value of β ranges from 0.0 to 1.0, with 0.0 representing a smooth crack (complete loss of shear transfer) and 1.0 representing a rough crack (no loss of shear transfer), **ANSYS**, **2007**.

The value of β used in many studies of reinforced concrete and composite steel-concrete structures, however, varied between 0.05 and 0.25, **Bangash**, **1989**; **Huyse**, **et al.**, **1994**; **Hemmaty**, **1998**; **Zebun**, **2006**. A number of preliminary analyses were attempted in this study with various values for the shear transfer coefficient within this range, but convergence problems were encountered at low loads with β less than 0.2. Therefore, the shear transfer coefficients for opened and closed cracks, used in this study, were equal to 0.2 and 0.22 respectively for all specimens.

2.3 Shear Connector

While the role of shear connectors (threaded bars) is divided into two parts: as transverse shear reinforcement in resisting shear forces inside the concrete layer (materially, modeled as shown in Fig. (2) and geometrically as discrete representation as shown in Fig. (4)) and as a shear connector in resisting horizontal and normal shear force between steel and concrete. A modified Push-out tests which were made by **Zebun**, **2006**, are adopted in this study. The modification in this test in comparison with the standard test concentrated on the use of steel tube-concrete slab-steel tube instead of concrete slab-steel (I-Section)-concrete slab (in the standard test) in order to

be more compatible than the standard test in modeling the steel-concrete-steel sandwich or double skin constructions. The concrete layer was reinforced with steel bars (according to **BS 5400-5:1979**), as shown in Fig. (5). With plain concrete layer similar to the sandwich slabs (the results of this group will be used in the finite element modeling of the sandwich specimens). Fig. (6) shows the average values of the load-slip relationship of the test.

Many different load-slip relationships for stud connectors have been proposed. Among these, an exponential model was presented by **Yam** and **Chapman**, **1968**. This is represented by the following function

$$Q = a\left(1-e^{-b\gamma}\right) \tag{5}$$

In which a and b are constants, and e is the base of natural logarithms. The constants a and b are chosen by trials to give the best fit with experimental curves. Alternatively, by choosing two points from the experimental curve so that the slip in the second point is twice its value at the first point then the constants can be defined as:

$$a = \frac{Q_1^2}{2 \cdot Q_1 - Q_2} \tag{6}$$

$$b = \frac{1}{\gamma_1} \log_e \left(\frac{Q_1}{Q_2 - Q_1} \right) \tag{7}$$

In which, subscripts 1 and 2 represent the points on the experimental load-slip curve for the provided shear connector. Fig. (6) shows a typical load-slip relationship (exponential formula).

The shear-slip model proposed by **Yam** and **Chapman**, **1968** for studs shear connector was adopted in the present study. The average values of the constants a and b of the push-out tests are (14.501) and (0.946) respectively.

3. FINITE ELEMENT MODEL

DSC slab is modeled as a non-linear three-dimensional model. The top and bottom steel plates are modeled using four-node shell elements SHELL143 each node have six degrees of freedom three translation and three rotation in X, Y, and Z direction and with a large strain formulation, whereas the concrete core is modeled using eight-node solid elements SOLID65 each nod have three degree of freedom (translation). To simulate the behavior of shear connectors which works as stirrups in resisting the vertical shear at concrete layer and transfer normal force between the concrete and steel plates LINK8 is used the 3-D spar element is a uniaxial tension-compression element with three degrees of freedom at each node: translations of the nodes in X, Y, and Z-directions. Partial interaction is assumed to occur between steel plates and concrete core COMPIN39 is used, in this study, to simulate the behavior of the shear connectors in resisting the horizontal shear between the concrete and the steel plates. The element is defined by two node points and a generalized force-deflection curve. In studying the contact between two bodies, the surface of one body is conventionally taken as a contact surface and the surface of the other body as a target surface. The contact surface is associated with the deformable body, and the target surface must be the rigid surface. TARGE170 is used to represent various 3-D target surfaces for the associated contact elements (CONTA174). Coulomb and shear stress friction is allowed. This element is used, in this study, to simulate the behavior of contact surface between

the concrete layer and steel plates (i.e. friction case between layers of the sandwich beam). The element is defined by one node.

4. EXAMPLES

The verification is done in order to check the validity and accuracy of the finite element procedure. Thus, two specimens with available experimental results have been analyzed here and the analytical results are compared.

4.1 Zebun Beams

A simply supported double skin composite beams, tested by **Zebun**, **2006** are two in a series of tested beams. The beams span (L_s) of 1020 mm and loaded with a central load (knife edge load, K.E.L.) applied and distributed across the entire width. Bars along the whole length were used as shear connectors and attached to the steel plates by nuts instead of welding; the nominal inner diameter of the bars was 6.2 mm (i.e. the bars penetrated fully through the concrete and the steel parts). Fabrication details of the tested beams are presented in Fig. (7). Pairs of connectors at each location were used, as shown in Fig. (8).

In the present study, the two chosen beams are designated as (B.1) and (B.3). The dimensions and load arrangement details of these beams are shown in Fig. (9). Table (1) illustrates the Nonlinear Parameters used for beams, and the material properties are given in Tables (2) and (3).

The three-dimensional finite element mesh for a quarter of the beam has been used by using ANSYS computer program, by taking the advantage of symmetry of the beam and loading Figs. (10), (11), and (12) show the pictures of a mesh of beams (B.1), and (B.3). In addition, details about the representation of structural component are done in Table (4).

The experimental and numerical results by Zebun, and numerical results obtained in the present study, for beams (B.1) and (B.3), are shown in Figs. (13), (14), (15), and (16). The mid-span externally applied load is plotted against the mid-span deflection. For these two beams, the failure load obtained by the experimental work and that predicted by the finite element solutions are listed in Table (5). It can be noted from Figures and Table (5) that the finite element solutions are in good agreement with the experimental results throughout the entire range of behavior.

4.2 Double Skin Composite Slabs

The close agreement has been observed between the finite element and experimental results for ultimate loads and load-deflection responses, for the two beams presented in the previous. The finite element model is thus found to be capable of predicting the behavior of DSC slabs accurately.

Other specimens having the same cross-section and span dimensions (1045 mm × 1045 mm × 87 mm), with a 75 mm thick concrete core sandwiched between two 6 mm thick steel plates will be studied under various effects of parameters. Threaded bars along both two directions are used as shear connectors and attached to the steel plates by nuts instead of welding. The nominal inner diameter of the bars is 6.2 mm, with effective length equal to the thickness of concrete layer used in each slab (i.e. the bars penetrated fully through the concrete and the steel parts). These slabs are simply supported on all sides and subjected to a uniform distributed load on the top surface.

The DSC slabs are modeled as a nonlinear three-dimensional structure. Owing to symmetry in geometry, loading and boundary conditions in the (ANSYS program), only a quarter of the DSC slab is modeled

It has been observed that the entire slab supported on two opposite edges had similar behavior under the applied loading. The failure type is mainly due to bending of the composite slab at midspan. Also bond (slip) failure between the concrete layer and steel plates caused fracture failure at the connector as the second failure.

In the present study, the slab is designated as (DSC1). The Details about material properties parameters for double skin composite slabs are listed in Table (6). It is the same material properties parameters which used for the panels in Chapter four the difference is in the dimensions and connectors spacing. Fig. (17) shows the boundary conditions of the quarter of the (DSC1) slab.

Details about the representation of structural component are listed in Table (7) and shown in Fig. (17). Table (1) illustrates the nonlinear parameters used for slabs.

The numerical results are shown in Fig. (18). The externally ultimate uniform distributed load is plotted against the central deflection. For this slab, the failure load predicted by the finite element solutions is (0.224 N/mm^2). Fig. (19) shows the variation of UY along a quarter of (DSC1).

The nonlinear analysis using Finite element method shows that DSC slabs have the very high load carrying capacity. This form of construction also exhibits good flexural characteristics and highly ductile behavior.

5. CONCLUSIONS

Depending on the numerical results obtained in this study, the following conclusions can be drawn:

1- A three-dimensional nonlinear finite element analysis was conducted to investigate the general behavior of sandwich members. Comparison between the experimental and the numerical results shows close agreement. The maximum difference ratio in ultimate load is less than 5% for the tested and analyzed sandwich beams.

2- Finite element analysis shows that DSC slabs have very high load carrying capacity. This form of construction also exhibits good flexural characteristics and highly ductile behaviour.

REFERENCES

- ANSYS, 2007 "*ANSYS Help*", Release 11, Copyright 2007.

- ACI Committee 318-14, "*Building Code Requirements for Structural Concrete* (318-14) and *Commentary* (318R-14)", American Concrete Institute, Michigan, USA, 2014.

- Bangash, M. Y. H., 1989 "*Concrete and Concrete Structures: Numerical Modelling and Applications*", Elsevier Science Publishers Ltd., London, England, Cited by Ref. [Kachlakev et al 2001].

- BS 5400, Part 5, 1979 "*Steel, Concrete and Composite Bridges-Code of practice for design of composite bridges*", British Standards Institution, London.

- Desayi, P. and Krishnan, S., 1964 "*Equation for the Stress-Strain Curve of Concrete*", Journal of the American Concrete Institute, Vol. 61, March 1964, pp. 345-350, Cited by Ref. [Kachlakev et al 2001].

- European Committee for Standardisation (CEN), Eurocode 4, "*Design of Composite Steel and Concrete Structures*", Part 1.1: General Rules and Rules for Buildings, DD ENV 1994-1-1, EC4.

- Gere, J. M. and Timoshenko, S. P., 1997 "*Mechanics of Materials*", PWS Publishing Company, Boston, Massachusetts, 1997.

- Kachlakev, D., Miller, T., and Yim, S., 2001 "*Finite Element Modelling of Reinforced Concrete Structures Strengthened with FRP Laminates*", Final Report, SPR 316, May 2001, 99 p.

- Huyse, L., Hemmaty, Y., and Vandewalle, L., 1994 "*Finite Element Modelling of Fiber Reinforced Concrete Beams*", Proceedings of the ANSYS Conference, Vol. 2, Pittsburgh, Pennsylvania, May 1994.

- Hemmaty, Y., 1998 "*Modelling of the Shear Force Transferred between Cracks in Reinforced and Fiber Reinforced Concrete Structures*", Proceedings of the ANSYS Conference, Vol. 1, Pittsburgh, Pennsylvania, August 1998.

- Yam, L. C. P. and Chapman, J. C., 1968 "*The Inelastic Behavior of Simply Supported Composite Beams of Steel and Concrete*", Proceeding of the Institution of Civil Engineers, Vol. 41, pp. 651-683.

- Zebun, M. A., 2006 "*Behavior and Strength of Steel-Concrete-Steel Sandwich Beams with Partial Shear Connection*", Ph.D. Thesis, Al-Mustansiriya University, Iraq-Baghdad, 194 p.

NOTATIONS

The major symbols used in this work are listed below; these and others are defined as they first appear. When duplication occurs, the used notation is clarified within the text.

E_c	Concrete modulus of elasticity
E_s	Steel modulus of elasticity
E_w	Steel Hardening Parameter
f_c'	Cylinder compressive strength of concrete
f_t	Splitting tensile strength of concrete
f_r	Concrete modulus of rupture
f_y	Yield strength of steel plate
f_u	Ultimate tensile strength of steel
G_s	Shear modulus of steel
h_c	Thickness of concrete layer
h_s	Thickness of steel plate
K_n	Normal stiffness of connector

L_s	Length of span
N	Number of shear connectors in a shear span
S-S	Simple supported
S_{stud}	Stud Spacing
U	Degree of freedom
UY	Deflection or vertical displacement
UX	Horizontal displacement in x-direction
X, Y, Z	Cartesian coordinate.
β_c , β_o	Shear transfer coefficient for closed & opened crack
ε	Strain
ε_o	Strain at ultimate compressive strength
μ	Coefficient of friction
υ	Poisson's ratio
υ_s	Poisson's ratio of steel
ϕ	Diameter
S_{stud}	Stud Spacing

Table 1. Nonlinear solution parameters used for beams.

μ	Coefficient of Friction	0.5*
α_1	Tension Stiffening Parameters	6*
α_2		0.6*
β_o	Shear Transfer Parameters	0.2*
β_c		0.22*
E_w	Steel Hardening Parameter (MPa)	4200*

*Assumed Values. The coefficient of friction μ is taken 0.5. $E_w = 0.02\, E_s$

Table 2. Material property parameters used for (B.1).

	Symbol	Definition	Value
Concrete	f'_c	Compressive Strength (MPa)	42.2
	E_c	Young's Modulus (MPa)	30532
	hc	Thickness (mm)	75
	f_r **	Tensile Strength (MPa)	4.95
	υ	Poisson's Ratio	0.2*
Top and bottom Steel Plate	f_y	Yield Stress (MPa)	255
	L,W,hs	Dimensions (length×width×thickness) (mm)	1100×100×6
	υ_s	Poisson's Ratio	0.3*
	E_s	Young's Modulus (MPa)	210000
Shear Connectors**	f_y	Yield Stress (MPa)	496
	ϕ	Diameter (mm)	6.2

	υ_s	Poisson's Ratio	0.3
	S_{stud}	Spacing (mm)	75
	E	Young's Modulus (MPa)	210000

Notes: $E_c = 4700\sqrt{f'c}$, * Assumed Values, ** Concrete modulus of rupture (flexural strength) by the prism of 100 mm × 100 mm × 500 mm and loaded at third points (Zebun study).

Table 3. Material property parameters used for (B.3).

	Symbol	Definition	Value
Concrete	f'_c	Compressive Strength (MPa)	43.9
	E_c	Young's Modulus (MPa)	31141
	hc	Thickness (mm)	75
	f_r*	Tensile Strength (MPa)	5.4
	υ	Poisson's Ratio	0.2
Upper and lower Steel Plate	f_y	Yield Stress (MPa)	255
	L, W, h_s	Dimensions (length×width×thickness) (mm)	1100×100×6
	υ_s	Poisson's Ratio	0.3
	E_s	Young's Modulus (MPa)	210000
Shear Connectors	f_y	Yield Stress (MPa)	496
	ϕ	Diameter (mm)	6.2
	υ_s	Poisson's Ratio	0.3
	S_{stud}	Spacing (mm)	150
	E	Young's Modulus (MPa)	210000

*Concrete modulus of rupture (flexural strength) by the prism of 100 mm x 100 mm x 500 mm and loaded at third points (Zebun study).

Table 4. Finite element representation of structural components.

Structural Component		Finite Element Representation	Element Designation in ANSYS	No. of element
Concrete		8-node Brick Element (3 Translation DOF per node)	SOLID 65	120
Interface	Shear Friction and Contact	Nonlinear Surface-to-Surface Interface Element	CONTA-174 & TARG170	120
	Dowel Action	2-node Nonlinear Spring Element with one Translation DOF per node	COMBIN-39	14*
				8**
Shear connector		2-node Discrete Element	3D-SPAR 8	28*

(Tensile Steel, Compressive Steel)	(3 Translation DOF per node)	(LINK-8)	16**
Steel plate	4-node Nonlinear plastic (3 Translation & 3 Rotation DOF Per node)	Shell 143	60

* For (B.1) ** For (B.3)

Table 5. Experimental and predicted failure loads for beams.

Specimens	Ultimate Load (N)		$\frac{P_u \text{ (Analytical)}}{P_u \text{ (Experimental)}}$	Failure mode	Error (%)
	Experimental	Analytical			
B.1	50000	49000	0.98	Connector fracture	2
B.3	27000	26730	0.99	Connector fracture	1

Table 6. material property parameters used for DSC slabs.

	Symbol	Definition	Value
Concrete	f'_c	Compressive Strength (MPa)	42.2
	E_c	Young's Modulus (MPa)	30532
	hc	Thickness (mm)	75
	f_r **	Tensile Strength (MPa)	4.95
	υ	Poisson's Ratio	0.2*
Top and bottom Steel Plate	f_y	Yield Stress (MPa)	255
	L,W,h_s	Dimensions (length×width×thickness) (mm)	1045×1045*6
	υ_s	Poisson's Ratio	0.3*
	E_s	Young's Modulus (MPa)	210000
Shear Connectors	f_y	Yield Stress (MPa)	496
	ϕ	Diameter (mm)	6.2
	υ_s	Poisson's Ratio	0.3
	S_{stud}	Connector Spacing (mm)	150
	E_s	Young's Modulus (MPa)	210000

Notes: $E_c = 4700\sqrt{f'c}$, * Assumed Values, ** Concrete modulus of rupture (flexural strength) by the prism of 100 mm x 100 mm x 500 mm and loaded at third points (Zebun study).

Table 7. Finite element representation of (DSC1) components.

Structural Component		Finite Element Representation	Element Designation in ANSYS	No. of element
Concrete		8-node Brick Element (3 Translation DOF per node)	SOLID 65	784
Interface	Shear Friction and Contact	Nonlinear Surface-to-Surface Interface Element	CONTA-174 & TARGE-170	784
	Dowel Action	2-node Nonlinear Spring Element with one Translation DOF per node	COMBIN-39	32
Shear connector (Tensile Steel, Compressive Steel)		2-node Discrete Element (3 Translation DOF per node)	3D-SPAR 8 (LINK-8)	64
Steel plate		4-node Nonlinear plastic(3 Translation &3 Rotation, DOF Per node)	Shell 143	392

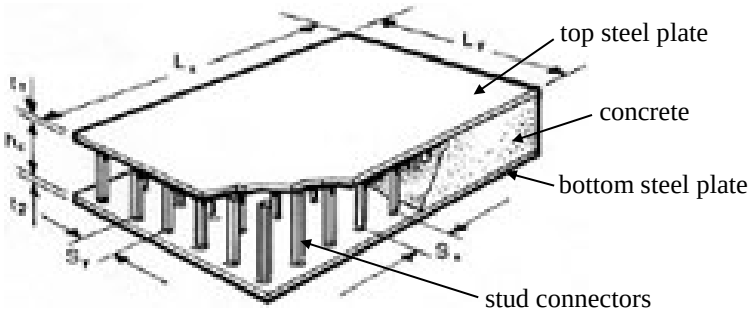

Figure 1. Double skin composite slabs.

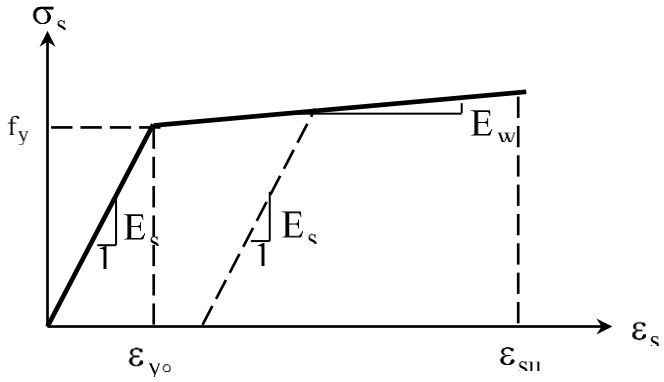

Figure 2. Bilinear stress-strain relationship.

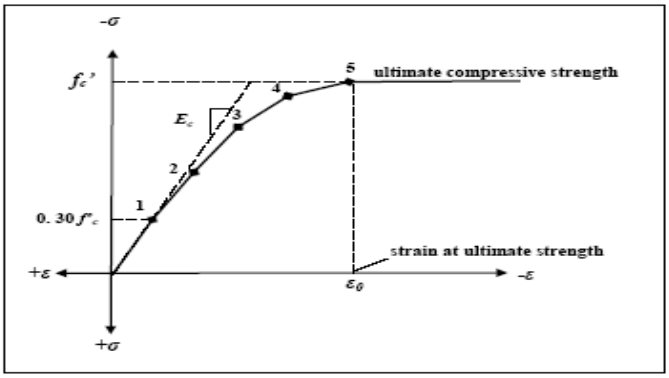

Figure 3. Simplified compressive uniaxial stress-strain curve for concrete.

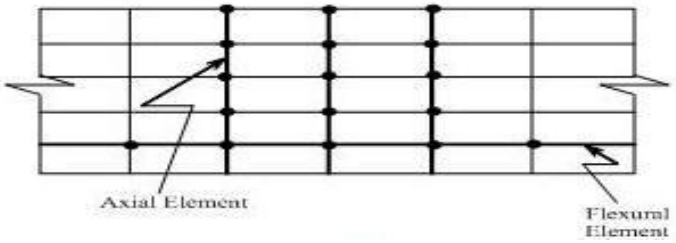

Figure 4. Discrete representation for shear connectors.

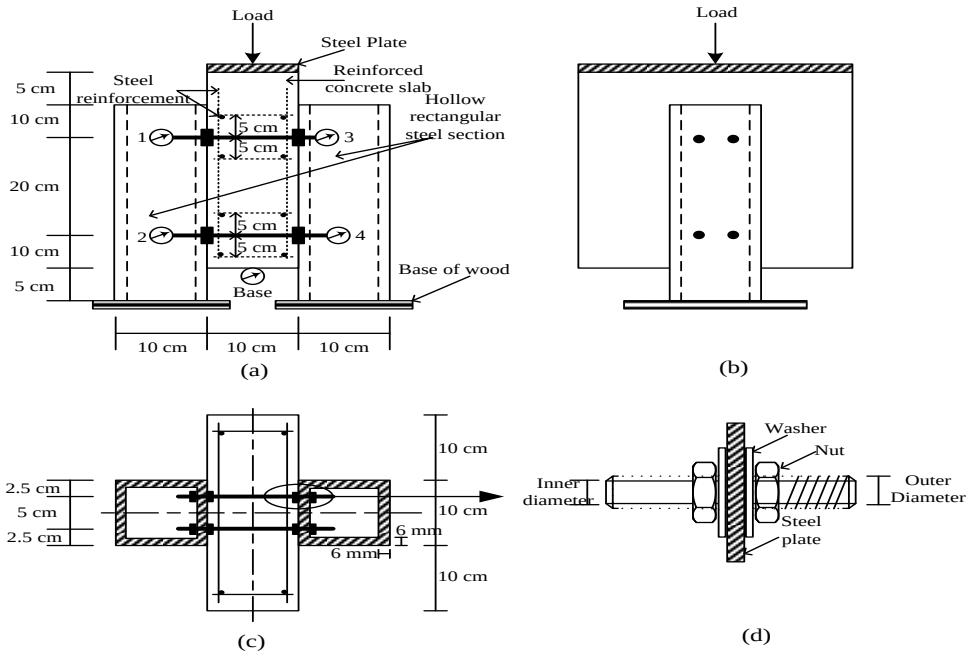

Figure 5. Dimensions and details of modified push-out test. (a) Front view. (b) Side view. (c) Top view. (d) Details of connection (magnified picture), **Zebun**, **2006.**

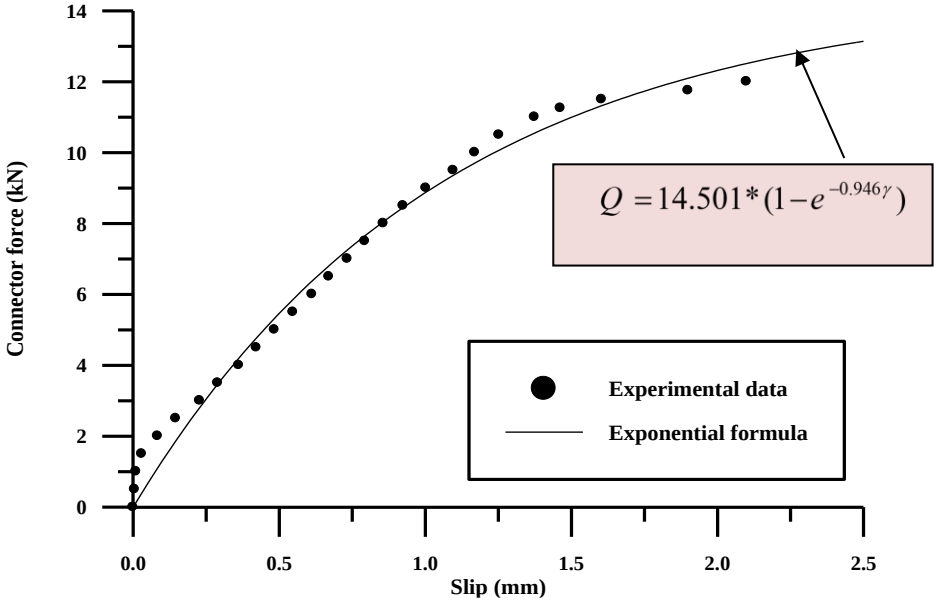

Figure 6. Load- slip relationship, **Zebun**, **2006**.

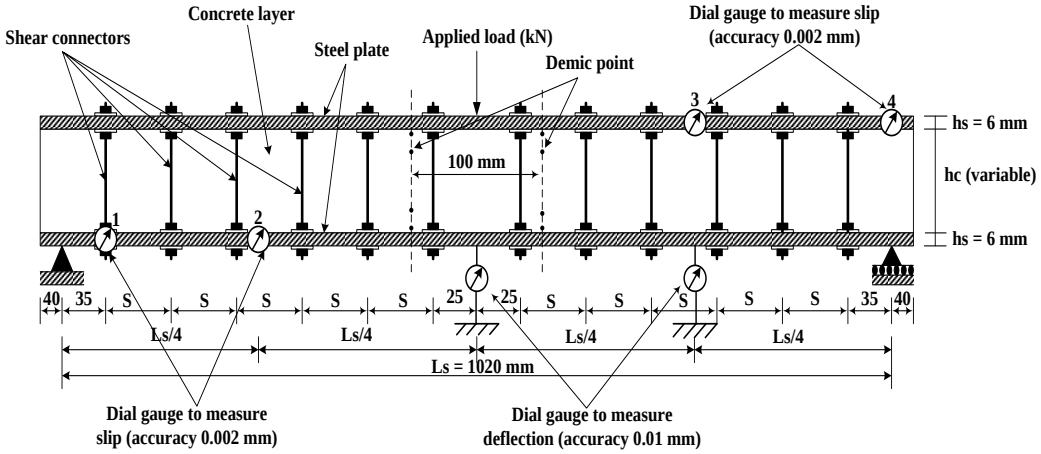

Figure 7. Fabrication details of test panels, **Zebun**, **2006**.

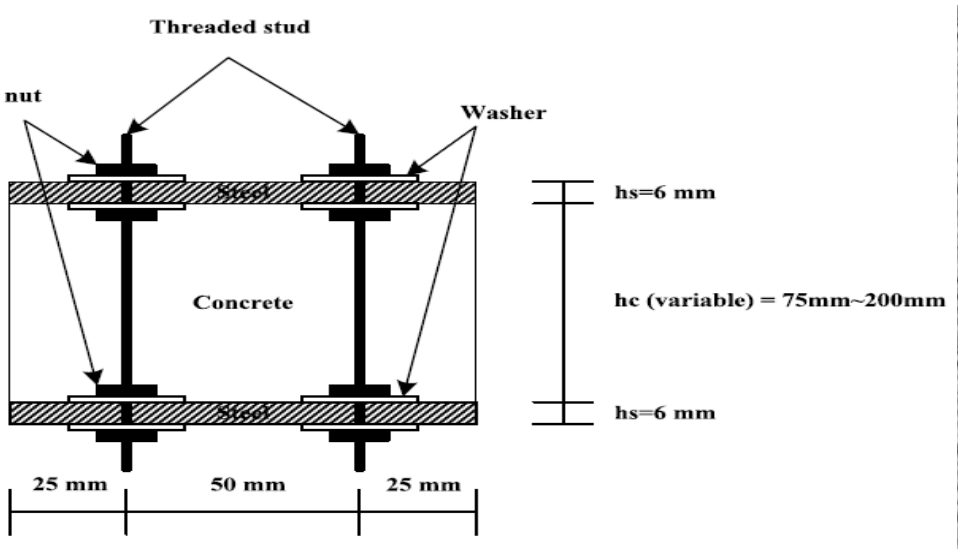

Figure 8. Cross section of SCSS beams, **Zebun**, **2006**.

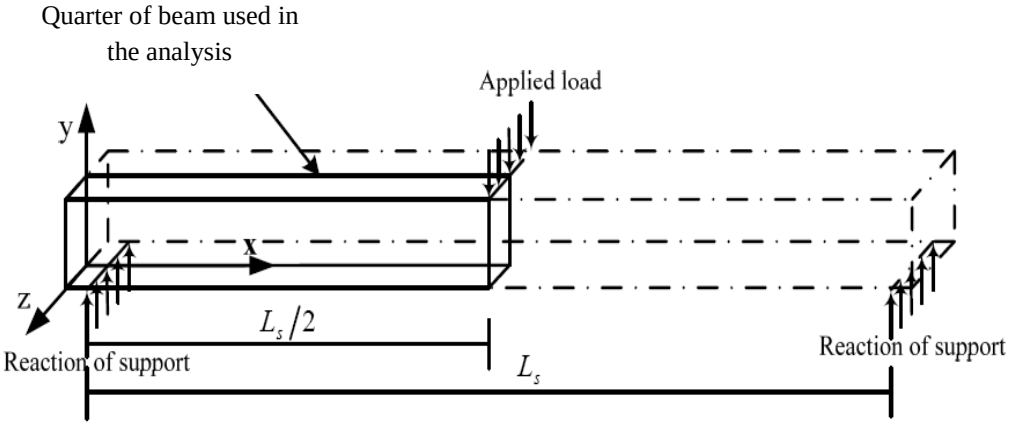

Figure 9. Dimensions and load arrangement details specimens.

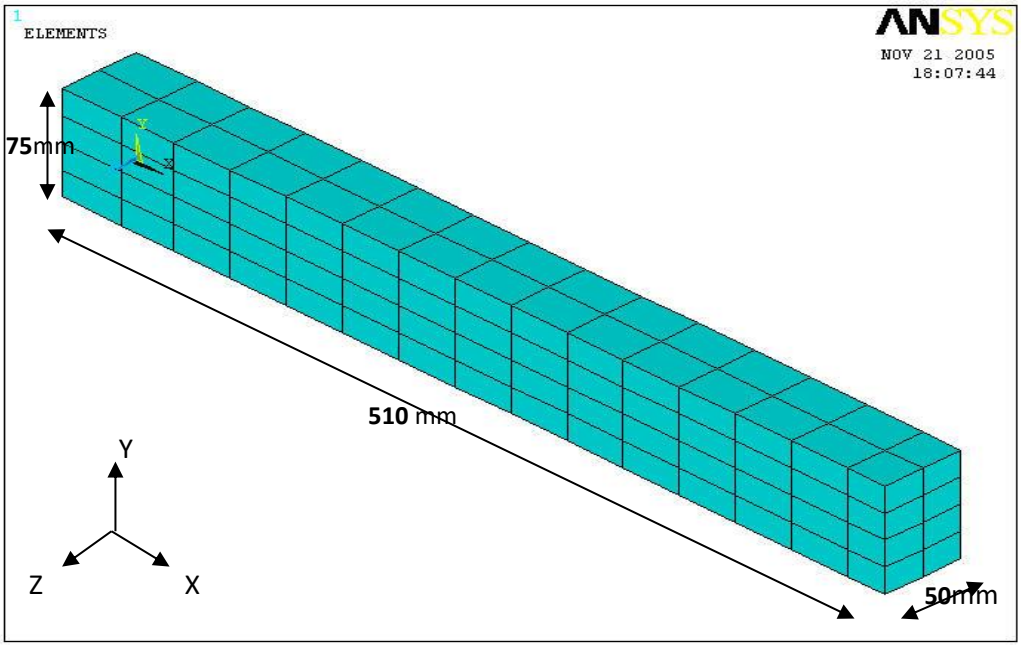

Figure 10. Mesh of quarter of beams.

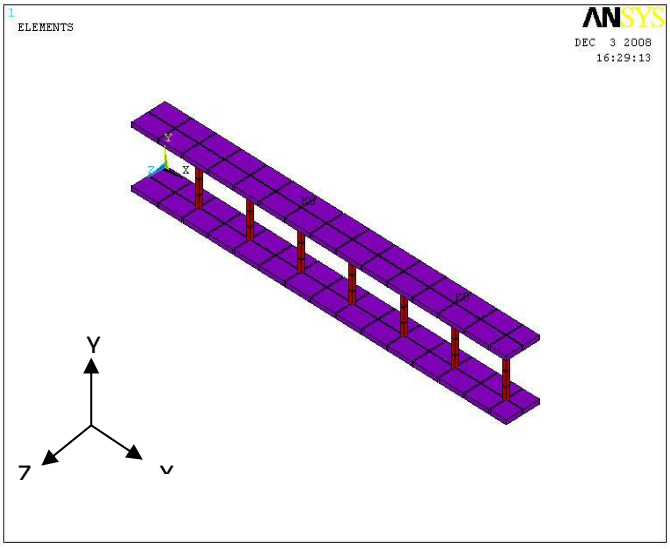

Figure 11. Mesh of LINK8 and SHELL143 for quarter (B.1).

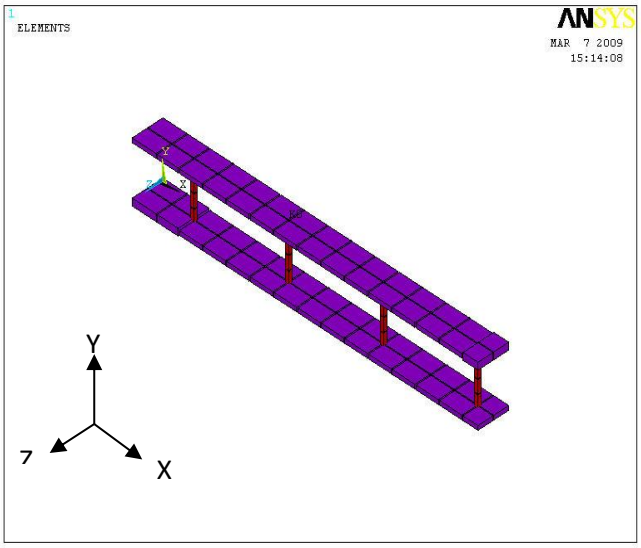

Figure 12. Mesh of LINK8 and SHELL143 for quarter (B.3).

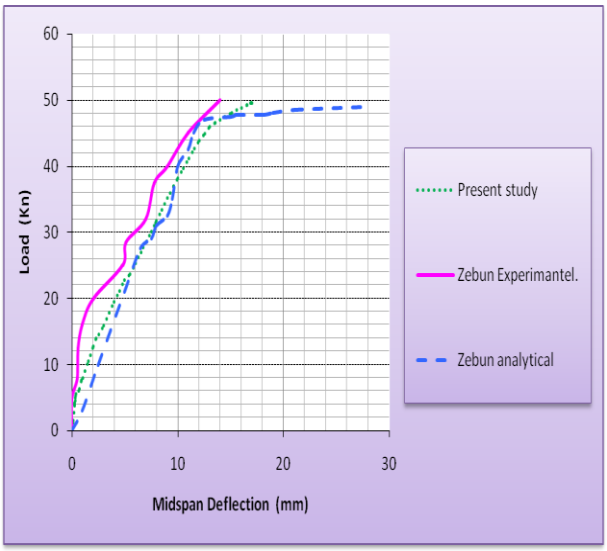

Figure 13. Load-Deflection response at mid-span of (B.1).

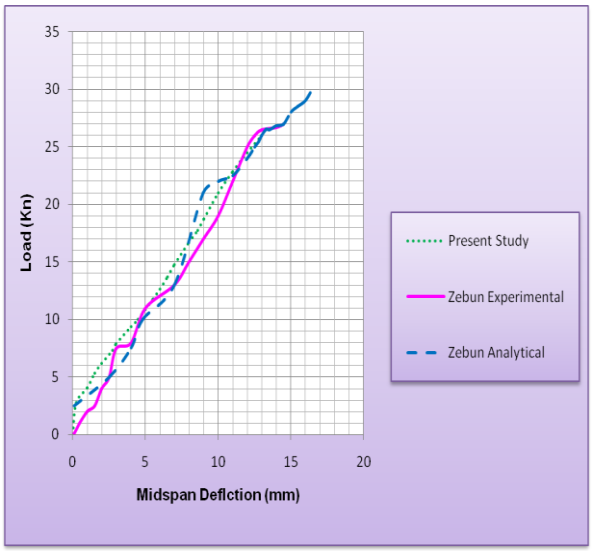

Figure 14. Load-Deflection response at mid-span of (B.3).

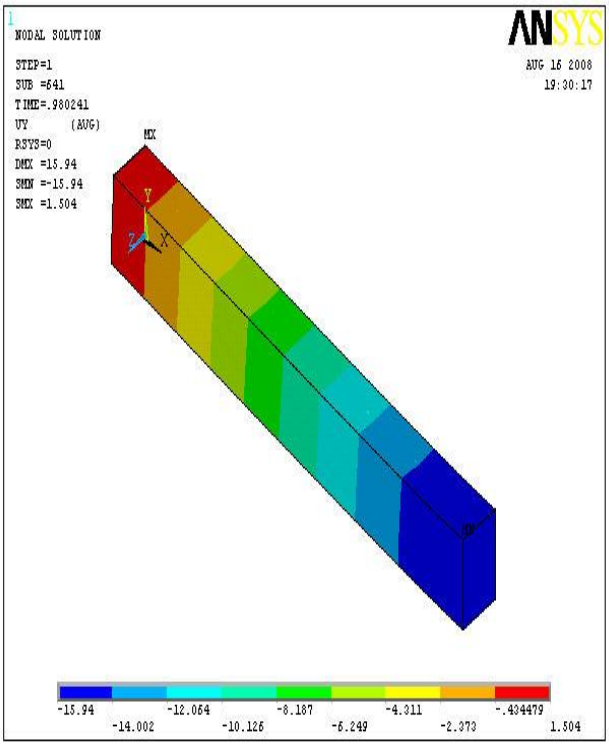

Figure 15. Variation of UY (vertical displacement) along quarter of B.1 at load equal to 98% of ultimate load**.**

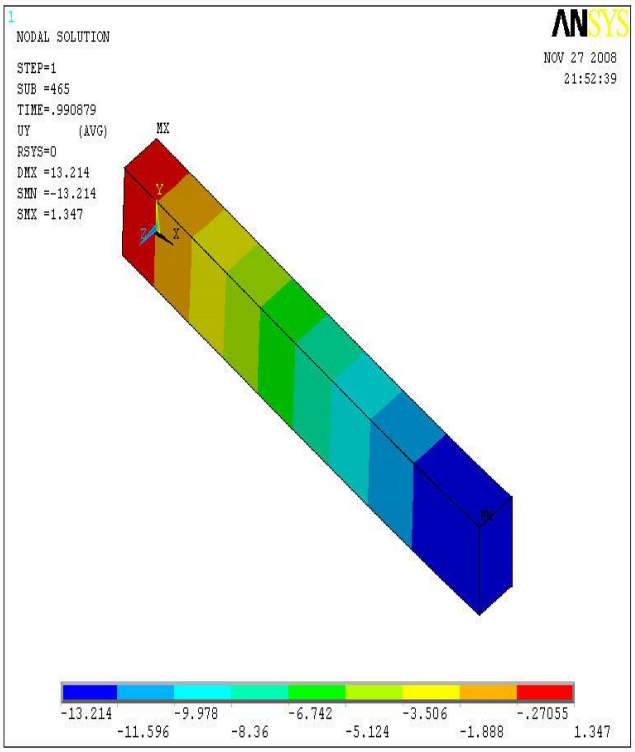

Figure 16. Variation of UY (vertical displacement) along quarter of B.3 at load equal to 99% of ultimate load. Note UY in mm.

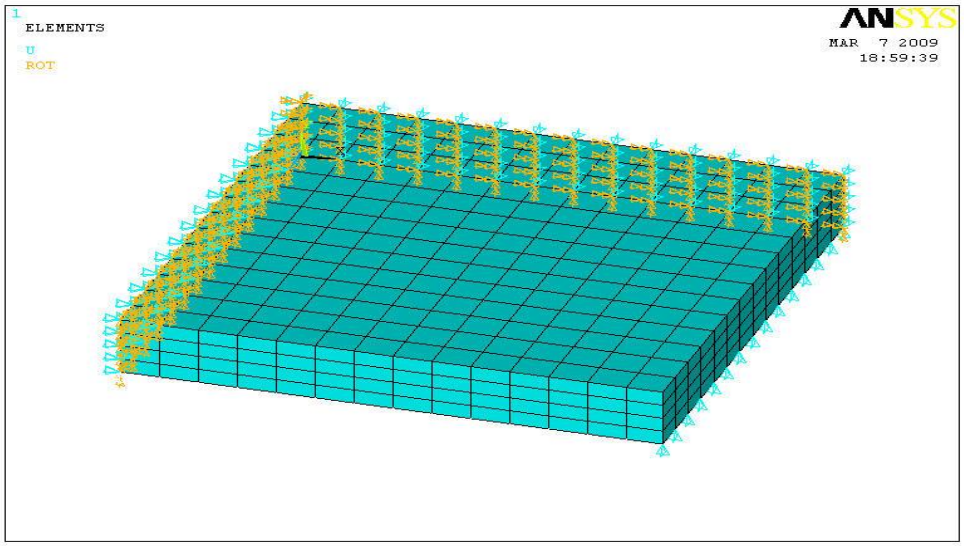

Figure 17. The boundary conditions of the quarter slab (DSC1).

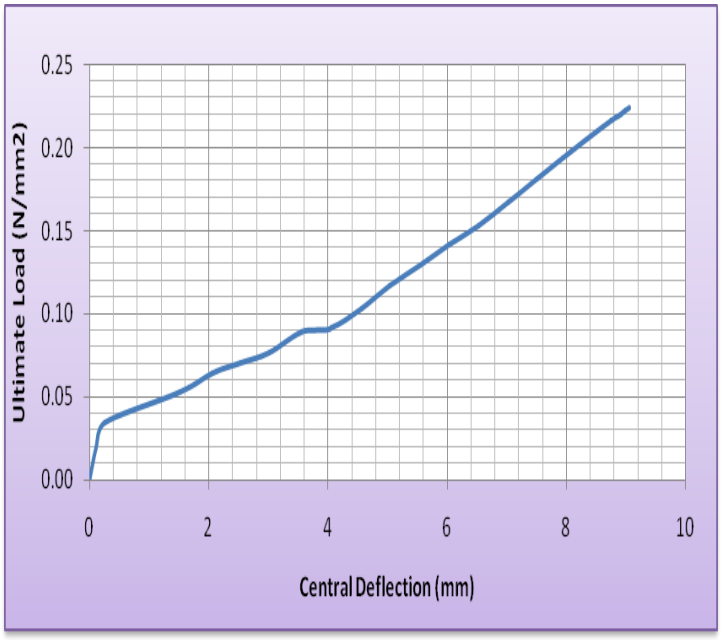

Figure 18. Load-deflection response of (DSC1).

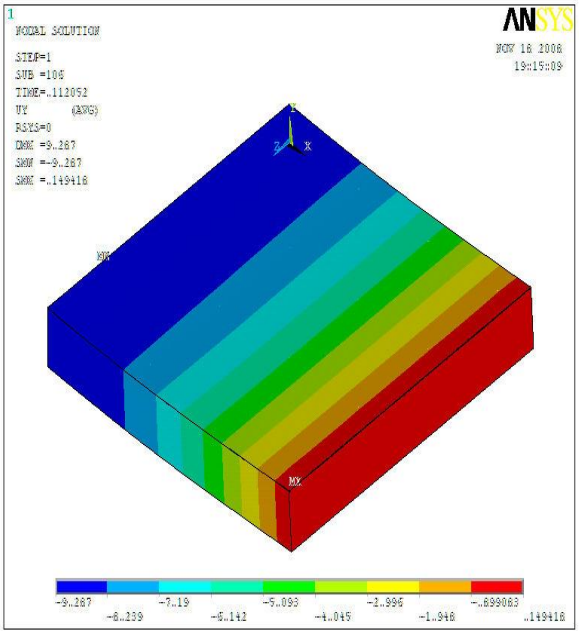

Figure 19. Variation of UY (vertical displacement) along quarter of DSC1.